From ions to data

Sally Marcher

Lecture Notes

December 23, 2024

1 Introduction

Mass spectrometry is a fundamental analytical technique employed in a multitude of scientific disciplines, including chemistry, biochemistry, pharmacy, and medicine, among others. These instruments are employed in a number of other capacities, including the elucidation of metabolic processes, the quality control of pharmaceuticals, and the examination of foodstuffs. From the 1950s to the present, mass spectrometry has undergone significant advancements, with ongoing developments occurring at a rapid pace.

In order to gain a fundamental comprehension of mass spectrometers, it is essential to acquire knowledge of the methodologies employed for the introduction of samples, the generation of ions, their mass analysis, and their detection. Additionally, it is crucial to understand the principles of data recording and the presentation of mass spectra. [11]

1.1 Aims and Scope of This document

In order to maintain a reasonable length and to ensure the document's presentability at 38c3, the scope has been significantly narrowed down to the essentials required to comprehend the fundamental principles of one specific type of instrumentation in mass spectrometry: the quadrupole mass filter.

A particular emphasis will be placed on the instrumentation and technical aspects, while maintaining a fundamental approach. For a more comprehensive examination of mass spectrometry at a broader level, please refer to the sources provided in this document.

1.2 A bit of history

In the years between 1950 and 1955, the concept of plane electric and magnetic multipole fields focusing particles in two dimensions, acting on the magnetic or electric dipole moment of the particles, was already under investigation. Lenses for atomic and molecular beams were conceived and realized (Friedburg and Paul, 1951; Bennewitz and Paul, 1954, 1955), resulting in a notable enhancement of the molecular-beam method for spectroscopy or for state selection. The lenses were also employed in the context of ammonia and the hydrogen maser (Townes, 1983).

The question "What happens if one injects charged particles, ions or electrons, in such multipole fields?" prompted the development of the linear quadrupole mass spectrometer. This instrument employs not only the focusing and defocusing forces of a high-frequency electric

quadrupole field acting on ions, but also exploits the stability properties of their equations of motion. This approach is analogous to the principle of strong focusing for accelerators, which had just been conceived. [1]

2 Ionization

Consider an ion that is brought into or generated within an electric field between two oppositely charged plates of a capacitor. Such an ion will be accelerated towards the plate of opposite charge. If the attracting plate has a (round) orifice or a slit, an ion beam is produced by this simple ion source. [10]

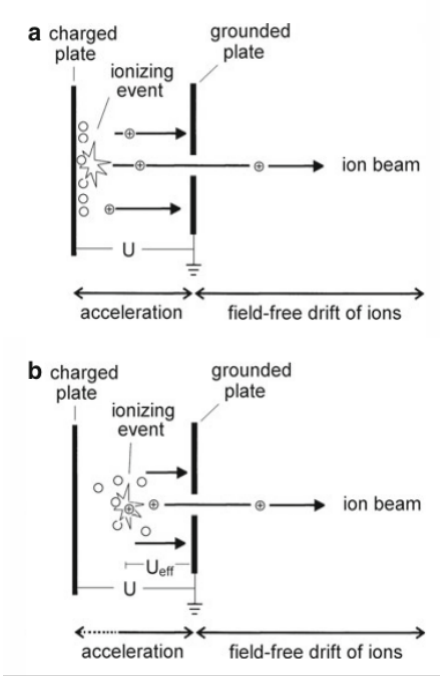

Figure 1: Simple single-stage ion sources (a) Ionization on the surface, (b) Gas phase ionization [10]

Depending on the sign of the charged plate and the ionization method used, this very simplified ion source can output differently charged particles. In practice, splitting the acceleration phase into several stages with ion optics (magnetic and electric fields) in between leads to higher extraction efficiency and better beam quality.

2.1 Electron Ionization

A beam of electrons is generated by thermionic emission from a resistively heated metal wire or filament typically made of rhenium or tungsten. This beam is then focused, making sure no electric fields from the electron source are leaking into the accelerating beam for ions, as this would lead to interfearances with the acceleration phase of the ions and could lead to overall substantial loss of resolution and mass accuracy of the mass spectrometer. [12]

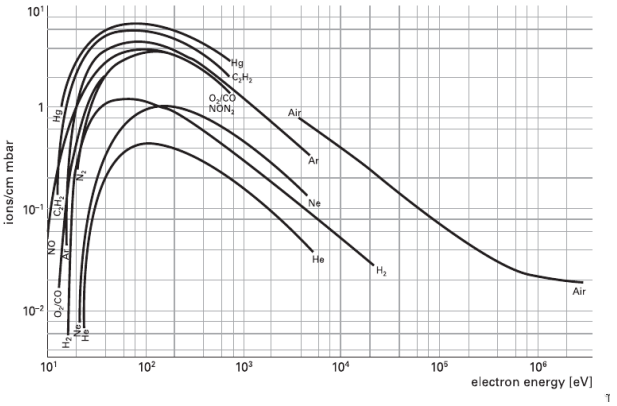

Figure 2: Ionization produced by electron impact, as a function of the electron energy. [3]

As can be seen in figure 2, the amount of ions obtained by the process of spraying electrons at particles depends largely on the average energy

of the electrons emitted. The optimal energy also depends on the type of gas, but generally energies of 50 to 200 eV are used in mass spectrometers. [7]

Unfortunately, more effects can occur, that must be taken into account when dealing with Electron Ionization [7], for more detail on each effect see [13]:

- Electron bombardment causes fragmentation of molecules in addition to ionization.
- Multiple ionization can also occur, for example Ar^{++} in addition to Ar^{+}.
- Electron stimulated desorption (ESD) results in additional ions and neutral.
- Outgassing of the surrounding walls caused by temperature rise induced by hot cathodes.

2.2 Electrospray Ionization

Electrospray ionization is one of the most frequently utilized ionization techniques in mass spectrometers. It is a highly "soft" ionization process, enabling the analysis of large, nonvolatile, chargeable molecules such as proteins and nucleic acid polymers [9].

This paper will examine one potential configuration of an electrospray ionization source as a case study. For a more comprehensive overview, please refer to the cited source [9].

2.2.1 Thermospray

The initial stage of the process, which is undertaken by the Thermospray apparatus, is the transfer of the analyte to a gas born aerosole. As illustrated in figure 3, the ion source of the API 2000 system is schematically represented. The chamber of the ion source is maintained at a relatively low vacuum level, which, strictly speaking, precludes the classification of this process as an API (atmospheric pressure ionization) method. This is done to improve Ion yield [16]. A flow of heated gas, with a temperature of approximately 500°C, is generated by the heated probe and employed for the evaporation of the solvent, containing the ionic analyte at very low concentration [9].

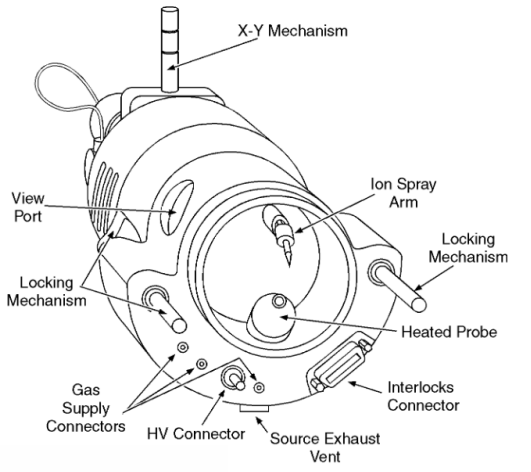

Figure 3: TurboIonSpray Inlet and Ion Source. [4]

The Ion Spray Arm is maintained at a high potential, facilitating the charging of the generated aerosol. During the subsequent evaporation process, the charge will gradually concentrate until the charge repulsion is greater than the surface tension (the Rayleigh limit). This will then result in a repetitive splitting of the charged droplets, ultimately generating a single ion, with the rest of the solvent evaporating. The aforementioned process is schematically represented in the top of figure 4.

The other model for this process is single

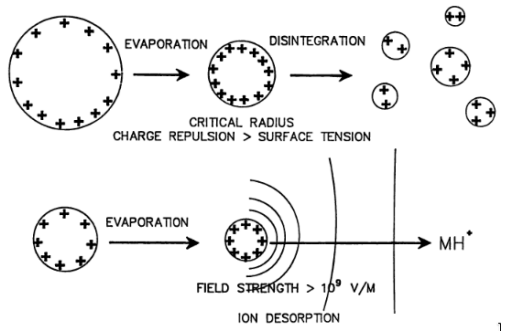

Figure 4: Schematic representation of the Charged Residue Model (CRM) and the Ion Desorption Model (IDM), also called Ion evaporation model (IEM) for ion formation [2]

ions escaping the droplet with increasing surface charge. This is illustrated in the bottom of figure 4. Analyte ions seperate in gas phase by desorbing individually [2].

A further popular model has emerged in recent times, offering an explanation of the macromolecular multiple charging process, particularly in unfolded proteins. This is known as the chain ejection model (CEM). When ESI is applied to unfolded proteins, the resulting ions are observed to be significantly more highly charged than those of folded proteins. This results in the unfolded protein being separated from the droplet. [16]

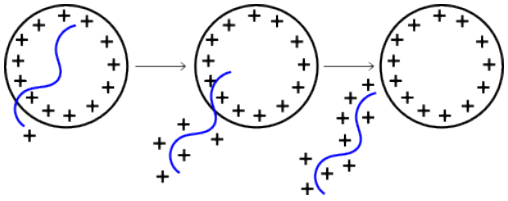

Figure 5: Schematic representation of the Charged Residue Model (CEM)

2.2.2 Vacuum Interface

The objective of the interface is to facilitate the evaporation of the solvent and the transfer of ions from a rough vacuum to a high vacuum. This process is typically accomplished in a series of sequential steps. Contemporary interfaces, as exemplified in figure 7, are all constructed around a fundamental design principle: a nozzle-skimmer system.

A jet of gas (curtain gas in figure 7) is introduced between the curtain and the orifice plate. Upon entering, the gas experiences a reduction in entropy due to the cooling effect of adiabatic expansion. Moreover, a portion of the thermal motion is transformed into directed flow by the nozzle-skimmer configuration. [9]

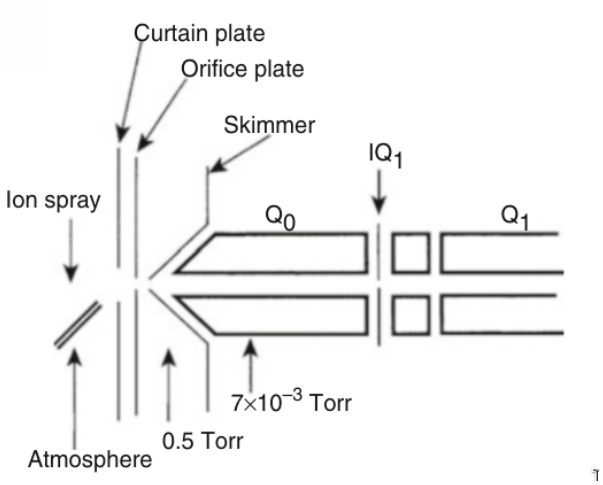

Figure 6: Electrospray interface setup for linear quadrupole and triple quadrupole instruments with 45° spray, heated countercurrent desolvation gas ("curtain gas"), orifice–skimmer setup for the first pumping stage, and RF-only quadrupole as ion guide in the second pumping stage. [9]

Subsequently, the beam passes through the skimmer electrode and is transmitted through Q0, an RF-only multipole. This indicates that the beam is not subjected to any filtering processes; rather, it is solely utilized for transmission to IQ1 (Interquad Lens 1). At this juncture, the beam enters an even higher vacuum level, where it may undergo filtration by the first quadrupole filter.

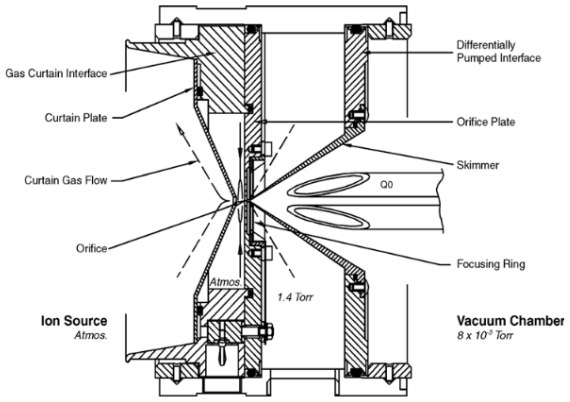

Figure 7: Vacuum Interface - Side View. [4]

2.3 Collision-Induced Dissociation

CID is done to fragment gaseous ions that were otherwise perfectly stable. This is done by introducing inert gas (like He, N_2, Ar) into the Vacuum and letting it collide with the ions.

The practical realisation of this process is usually done via a collision cell, within the collision cell the pressure is significantly higher than in the surrounding vacuum. This is done by having small entrance and exit slits for the ions and introducing the gas with a controlled flow, creating a differentially pumped region.

It is evident that the collision of gas molecules with the ion beam inevitably results in a reduction of the beam intensity. This phenomenon is directly correlated with the pressure within the collision cell. As the pressure within the chamber is increased, the probability of multiple collisions also rises. This is illustrated in figure 9.

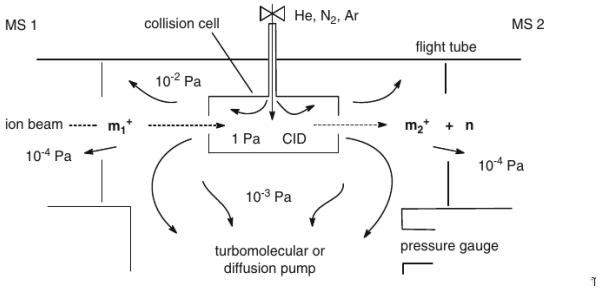

Figure 8: Schematic of a collision cell for CID. [14]

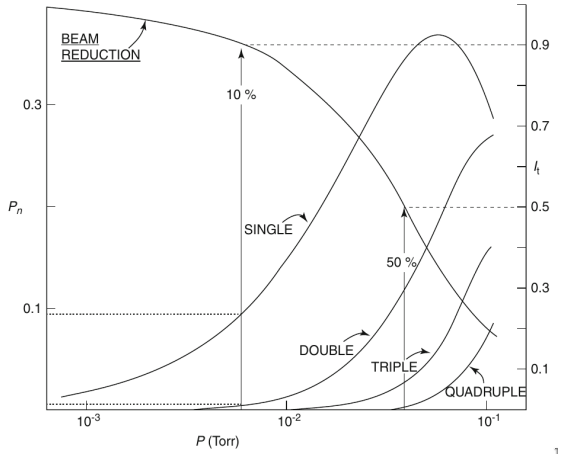

Figure 9: Total collision probability Pn (left ordinate) and fractions of single, double, triple, and quadruple collisions vs. collision gas pressure. [14]

Following the generation of the fractional ions, these are subjected to further filtration through a mass filter of some kind, such as a quadrupole.

3 Quadrupole mass filter

In this paragraph, I have primarily adhered to [1], supplementing it with additional commentary to enhance my comprehension of the intermediate stages.

In order to constrain a mass in position, it is necessary to apply a force that is proportional to the position vector and oriented in the opposite direction.

$$\vec{F} = -c \cdot \vec{r} \tag{1}$$

where:
$\vec{F}$...force acting on the mass
c ...constant
$\vec{r}$ ...position vector

To facilitate comprehension, it is helpful to envision a one-dimensional scenario. In such a case, a parabolic potential function would be a suitable solution.

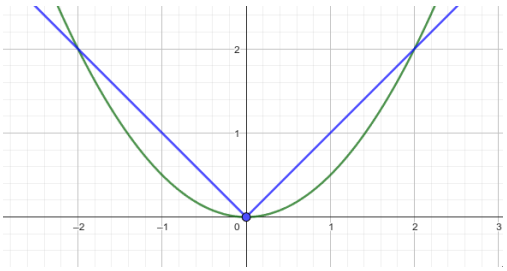

Figure 10: Visualization of the potential (green) and the absolute value of the Force (blue)

If we expand this principle into a 3 dimensional space we can thus assume a potential as follows.

$$\Phi \propto (\alpha \cdot x^2 + \beta \cdot y^2 + \gamma \cdot z^2) \tag{2}$$

where:
Φ ...potential
α, β, γ...constants
x, y, z ...cartesian coordinates

In order to achieve an equal, one may choose to employ the geometric context in a relatively effortless manner:

$$\Phi = \frac{\Phi_0}{2 \cdot {r_0}^2}(\alpha \cdot x^2 + \beta \cdot y^2 + \gamma \cdot z^2) \tag{3}$$

where:
Φ_0...potential at electrode
r_0 ...distance from center to the electrode

The Laplace Condition $\Delta\Phi = 0$ applied to equation (2) expands to:

$$\Delta\Phi = \nabla^2\Phi = \frac{\partial\Phi^2}{\partial^2 x} + \frac{\partial\Phi^2}{\partial^2 y} + \frac{\partial\Phi^2}{\partial^2 z} = 0 \tag{4}$$

Note: The Laplace condition can be derived from Gauss's Law, which states that "the flux of the force through any closed surface is proportional to the net charge contained within that surface" when a conservative force is assumed, as was done in reference to equation (1), and when the assumption is made that there are no charges present in empty space. [6]

Differenciating equation (4) leads to:

$$\alpha + \beta + \gamma = 0 \tag{5}$$

The equation has an infinite number of solutions; however, for the purposes of this discussion, we will focus on two of them and provide context for each.

(i) $\alpha = 1, \beta = 0, \gamma = -1$

(ii) $\alpha = \beta = 1, \gamma = -2$

(i) in equation (3) leads to

$$\Phi = \frac{\Phi_0}{2 \cdot {r_0}^2}(x^2 - z^2) \tag{6}$$

where:
Φ ...potential
Φ_0 ...potential at electrode
x, z...cartesian coordinates
r_0 ...distance from center to the electrode

This resulted in the 3D field being reduced to an even 2D field along the y-axis. This is the fundamental principle underlying the quadrupole mass filter, and a more detailed examination will be provided subsequently.

(ii) in equation (3) leads to

$$\Phi = \frac{\Phi_0}{2 \cdot {r_0}^2}(x^2 + y^2 - 2 \cdot z^2) \tag{7}$$

Converted to cylindrical coordinates ($x^2 + y^2 = r^2, 2 \cdot {z_0}^2 = r_0^2$):

$$\Phi = \frac{\Phi_0 \cdot (r^2 - 2 \cdot z^2)}{{r_0}^2 + {z_0}^2} \tag{8}$$

where:
r, z...cylindrical coordinates
r_0 ...distance from center to the electrode

This constitutes the fundamental principle underlying electromagnetic traps, a topic that may warrant further discussion at a future date.

For this document we'll focus on equation (6).

The potential, designated as Φ_0, represents the applied potential to the electrode of the mass filter. It is composed of a static voltage of amplitude U and an alternating voltage of amplitude V with angular frequency ω. This function is an alternating function of time.

$$\Phi_0(t) = U + V \cdot cos(\omega \cdot t) \tag{9}$$

where:
$\Phi_0(t)$...total potential applied between electrodes
U ...static potential
V ...amplitude of alternating potential
ω ...angular frequency

The electric field is the first derivative of the electric potential. [8]

Thus we can partially derive equation (6) in order to get the electric field components in x and z direction.

$$E_x = -\frac{\partial \Phi}{\partial x} = -\frac{\Phi_0(t)}{r_0^2} \cdot x \tag{10}$$

where:
E_x...electric field x component

Same for E_z.

$$E_z = -\frac{\partial \Phi}{\partial z} = \frac{\Phi_0(t)}{r_0^2} \cdot z \tag{11}$$

where:
E_z...electric field z component

If you are following along, you may already have a significant question: where does the "mass to charge ratio" originate from that is repeatedly referenced in mass spectrometry discussions ($\frac{q}{m}$)? This is related to the subsequent step:

The force acting on a charged mass is the masses charge multiplied with the electric field. [8]

$$\vec{F} = q \cdot \vec{E} \tag{12}$$

Applying Newton ($F = m \cdot a$) to this formula leads to:

$$a = \frac{q \cdot E}{m} \tag{13}$$

We can now insert each equation (10) and equation (11) into equation (13) and use $a = \frac{d^2x}{dt^2}$

$$\frac{d^2x}{dt^2} = -\frac{q \cdot \Phi_0(t)}{m \cdot r_0^2} \cdot x \tag{14}$$

$$\frac{d^2z}{dt^2} = \frac{q \cdot \Phi_0(t)}{m \cdot r_0^2} \cdot z \tag{15}$$

Inserting equation (9) and re-arringing the formulas lead to the differential equations for the path through the mass filter.

$$\frac{d^2x}{dt^2} + \frac{q}{m \cdot r_0^2} \cdot (U + V \cdot cos(\omega \cdot t)) \cdot x = 0 \tag{16}$$

$$\frac{d^2z}{dt^2} - \frac{q}{m \cdot r_0^2} \cdot (U + V \cdot cos(\omega \cdot t)) \cdot z = 0 \tag{17}$$

The resolution of this differential equation presents a significant challenge. Differential equations of this form are designated as "Mathieu equations" and are characterized by the following general form:

$$\frac{d^2x}{d\tau^2} + (a + 2q \cdot cos(2\tau))x = 0 \tag{18}$$

By comparing with equation (16) we get:

$$a = \frac{4qU}{mr_0{}^2\omega^2}, q = \frac{2qV}{mr_0{}^2\omega^2}, \tau = \frac{\omega t}{2} \tag{19}$$

The solution to this differential equation is not a straightforward one and requires an understanding of advanced mathematical concepts. It would be advisable to refer to the derivation of the stability diagram of Mathieu's equation, as presented in reference [5].

Similarly, as illustrated in the ideal Paul trap described in reference [5], the stability diagram for a quadrupole can be obtained with stability in the X-axis, Y-axis, or both in the intercepting areas.

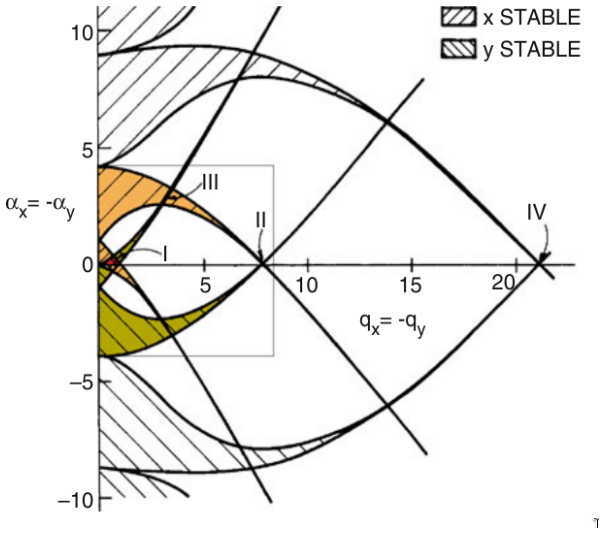

Figure 11: Stability diagram for a linear quadrupole analyzer showing four stability regions [10]

The area (I) in figure 11 is of interest for quadrupole mass filters. By maintaining a constant ratio of a/q while "scanning along the scan line," it is possible to achieve mass separation. The a/q ratio is selected in such a way that the xy-stability region is reduced to a single point, which is marked in figure 12. [10]

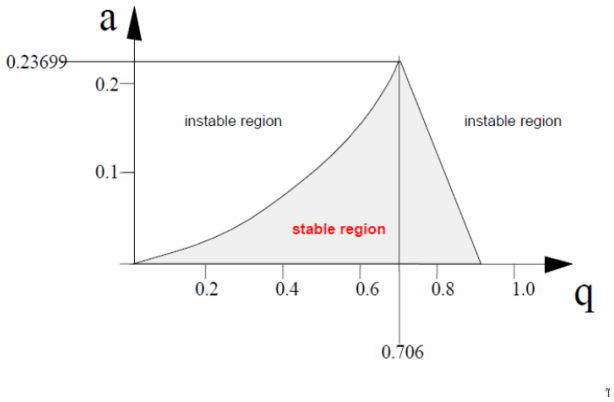

Figure 12: Stability diagram section (1) in figure 11 [7]

The extension of the principle outlined in figure 12 to encompass multiple masses results in the phenomenon illustrated in figure 13.

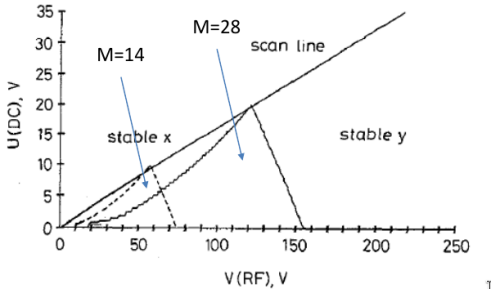

Figure 13: Stability diagram showing peak condition for nitrogen(N_2^+) at U = 20V, V = 123.5 V [Filter radius (r_0) = 2.75mm and frequency (f) = 2MHz] [7]

3.1 Resolving Power

It is not possible to increase the a/q ratio indefinitely; at a certain point, no further masses will be able to pass the mass filter. The ultimate limit is determined by the accuracy of the manufacturing process.

Theoretically, the optimal shape for the mass spectrometers' rods would be hyperbolic rods, as assumed in equation (3). In practice, however, most mass spectrometers use circular rod surfaces, which facilitates manufacturing but results in a loss of resolution. [10]

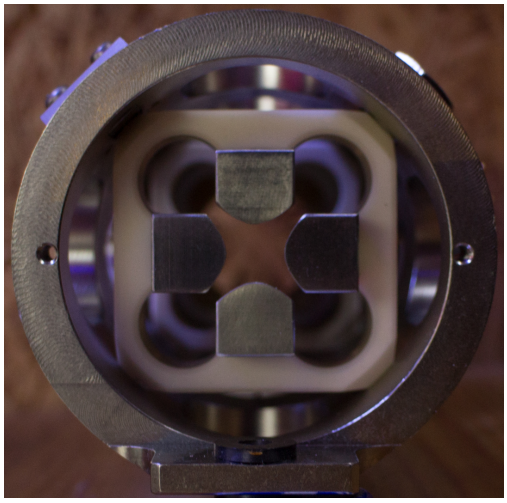

Figure 14: Linear quadrupole with hyperbolic rods.

4 Detection

The simplest detector is the faraday cup. In other terms, it's an electrode where the ion, when in contact with the metal surface, can deposit its charge. [10]

Without any path to go to, the charge would just accumolate until no Ion can deposit any more charge, thus a high impeadance resistor with a path to ground is connected, a deposited charge can now be detected as a voltage spike and can then be further amplified.

The downside to this method is the need of very high gain and exact amplifiers, thus secondary electron emission is used instead.

4.1 Secondary electron emission

You can imagine a metal or semiconductor as a ball pit filled with balls representing electrons. Picture someone throwing a ball into the pit with enough energy. If the ball is thrown hard enough, it can cause several balls to be ejected from the pit, not just the one that was thrown in. In this analogy, the walls of the ball pit represent the electron work function—the energy barrier that electrons need to overcome to escape the material. This is analogous to secondary electron emission, where a single high-energy primary electron can excite multiple secondary electrons, ejecting them from the surface of the metal or semiconductor.

In figure 15, E_F represents the potential for electrons in the valence band, while Φ_V is the energy required to elevate an electron above E_{VAC}. Once this energy is provided, the electron can overcome the potential barrier (the hill) and escape.

A high-energy electron entering the system possesses significantly more energy than $E_{VAC} -$

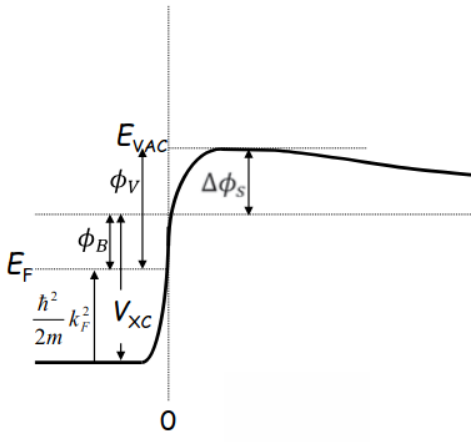

Figure 15: Potential diagram as a function of the distance between the surface and the final position of the electron [17]

E_F. As a result, it can transfer sufficient energy to multiple electrons within the material, exciting them above the E_{VAC} potential. This allows these electrons to overcome the energy barrier and escape.

4.2 Discrete Dynode Electron Multipliers

If an electrode opposite to the location of emission is held at more positive potential, all emitted electrons will be accelerated towards and hit that surface where they in turn cause the release of several electrons each. The avalanche of electrons produced over 12–18 discrete dynode stages held at about 100 V more positive potential each causes an electric current large enough to be detected by a sensitive preamplifier. Such a detector is called secondary electron multiplier. [10]

4.3 Continous Dynode Electron Multipliers

The same effect can be achieved using a channel instead of discrete dynodes. These channel electron multipliers are often cheaper to manufacture. In such devices, the material of the dynode drops a voltage of approximately 2 kV through a resistive coating. The gain in these electron tubes depends on the length-to-diameter ratio, with the optimum typically being between 40 and 80.

To address issues with generating positively charged ions at gains above 10^4, which interfere with ions at the input due to electron emission, a curved design was developed. The curved structure reduces the free path for ion acceleration, thereby suppressing noise caused by this so-called ion feedback. These curved multipliers can achieve gains of up to 10^8.

4.4 Post-acceleration and Conversion Dynode

One of the challenges associated with both of the previously mentioned electron multipliers is the discrimination between slower and faster ions. Practically, this results in reduced sensitivity for ions with higher mass or when operating the mass spectrometer at a lower accelerating voltage.

To address this issue, a post-acceleration conversion dynode is employed. This dynode is set to a high potential—positive or negative, depending on the type of ions—of up to 30 kV. It is constructed from a robust material and serves to convert incoming ions into secondary electrons or ions, which can then be directed into the SEM or CEM (Continous Dynode Electron Multipliers) for detection. Additionally, neutrals and photons are prevented from reaching the detector if the conversion dynode is positioned out of the line of sight. [10]

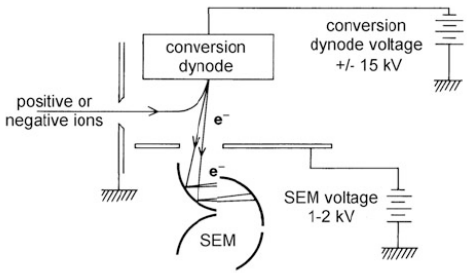

Figure 16: Detector configuration with conversion dynode [11]

5 Interpretation of Data

Given my limited practical experience with mass spectrometers as analytical tools, this example will be relatively simple.

In this example, an attempt will be made to analyze coffee in order to detect any peaks that may signify caffeine. It is of the utmost importance to prepare the sample correctly, as any contamination can result in a clogged injection tube. In this case, the coffee was diluted 1:500 with water and analyzed by direct injection.

The utilisation of HPLC (high-pressure liquid chromatography) would undoubtedly prove advantageous in this process; however, the current setup does not include this capability. Consequently, direct injection was the sole viable option.

The initial step was a Q1 scan. On the x-axis, the m/q ratio is observed, while on the y-axis, the detection rate, an arbitrary unit, is plotted. It is anticipated that a maximum will

be observed at m/q=195.2, as referenced in [15], due to the molecular mass of caffeine (194.19 amu) and its ionisation behaviour. The mass spectrometer is currently operating in positive ionization mode, which results in the addition of a proton (H^+) to the molecule under observation, effectively increasing its mass by one atomic mass unit (amu).

This observation will not, however, constitute definitive proof, as there may be other molecules present in the coffee with the same exact m/q ratio.

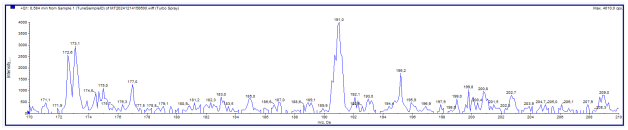

Figure 17: Q1 Scan mass spectra

As anticipated, a peak at 195.2 was identified. As a definitive answer, it can be stated that this is indeed caffein the disruption cell that can be engaged, while fixating Q1 at m/q 195.2. Consequently, instead of a Q1 scan, a Q3 scan will be conducted. This is the mass filter that occurs after the disruption cell, following the fragmentation of ions. In accordance with the findings presented in reference [15], it is anticipated that a peak will be observed at m/q 138.0.

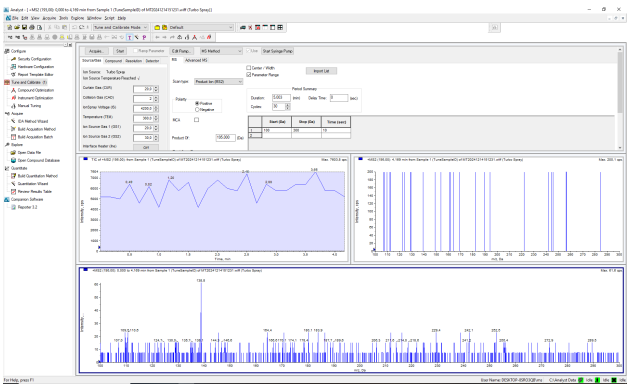

Figure 18: Q3 Scan mass spectra, collision energy: 30 eV.

Following a four-minute runtime, a peak was observed at m/q 138.8. While the peak was not particularly large in terms of signal strength, it was nevertheless indicative of the presence of caffeine in the coffee sample.

References

[1] Wolfgang Paul. "Electromagnetic traps for charged and neutral particles". In: *Rev. Mod. Phys.* 62 (3 1990), pp. 531–540. DOI: 10.1103/RevModPhys.62.531. URL: https://link.aps.org/doi/10.1103/RevModPhys.62.531.

[2] A.P. Snyder, American Chemical Society. Division of Analytical Chemistry, and American Chemical Society. Meeting. *Biochemical and Biotechnological Applications of Electrospray Ionization Mass Spectrometry*. ACS symposium series. American Chemical Society, 1996. ISBN: 9780841233782. URL: https://books.google.at/books?id=u7PwAAAAMAAJ.

[3] Pfeiffer Vacuum GmbH. *Mass spectrometer*. https://www.researchgate.net/profile/Yuriy_Kudriavtsev/post/Can_quadrupole_mass_analyzer_works_in_the_pressure_of_10Pa/attachment/59d63ac779197b8077997d72/AS:407444925763584@1474153848291/download/Pfeiffer+Mass+Spectrometer+Catalog+2005+-+2007.pdf. Accessed: 2024–12-09. 2005.

[4] MDS Sciex and Applera Corporation. *API 2000 LC/MS/MS System, Service Manual*. https://archive.org/details/manualzilla-id-6019978. Accessed: 2024–12-10. 2005.

[5] Timothy Jones. *MATHIEU'S EQUATIONS AND THE IDEAL RF-PAUL TRAP*. http://einstein.drexel.edu/ tim/open/mat/mat.pdf. Accessed: 2024–12-15. 2008.

[6] David Skinner. *Mathematical Methods*. https://www.damtp.cam.ac.uk/user/dbs26/1BMethods/Laplace.pdf. Accessed: 2024–12-09. 2015.

[7] Paolo Chiggiato Berthold Jenninger. *CAS tutorial on RGA Essential Knowledge*. https://indico.cern.ch/event/565314/contributions/2285748/attachments/1467497/2273711/RGA_tutorial-theory.pdf. Accessed: 2024–12-09. 2017.

[8] Wolfgang Demtröder. "Elektrostatik". In: *Experimentalphysik 2: Elektrizität und Optik*. Berlin, Heidelberg: Springer Berlin Heidelberg, 2017, pp. 1–40. ISBN: 978-3-662-55790-7. DOI: 10.1007/978-3-662-55790-7_1. URL: https://doi.org/10.1007/978-3-662-55790-7_1.

[9] Jürgen H. Gross. "Electrospray Ionization". In: *Mass Spectrometry: A Textbook*. Cham: Springer International Publishing, 2017, pp. 721–778. ISBN: 978-3-319-54398-7. DOI: 10.1007/978-3-319-54398-7_12. URL: https://doi.org/10.1007/978-3-319-54398-7_12.

[10] Jürgen H. Gross. "Instrumentation". In: *Mass Spectrometry: A Textbook*. Cham: Springer International Publishing, 2017, pp. 151–292. ISBN: 978-3-319-54398-7. DOI: 10.1007/978-3-319-54398-7_4. URL: https://doi.org/10.1007/978-3-319-54398-7_4.

[11] Jürgen H. Gross. "Introduction". In: *Mass Spectrometry: A Textbook*. Cham: Springer International Publishing, 2017, pp. 1–28. ISBN: 978-3-319-54398-7. DOI: 10.1007/978-3-319-54398-7_1. URL: https://doi.org/10.1007/978-3-319-54398-7_1.

[12] Jürgen H. Gross. "Practical Aspects of Electron Ionization". In: *Mass Spectrometry: A Textbook*. Cham: Springer International Publishing, 2017, pp. 293–324. ISBN: 978-3-319-54398-7. DOI: 10.1007/978-3-319-54398-7_5. URL: https://doi.org/10.1007/978-3-319-54398-7_5.

[13] Jürgen H. Gross. "Principles of Ionization and Ion Dissociation". In: *Mass Spectrometry: A Textbook*. Cham: Springer International Publishing, 2017, pp. 29–84. ISBN: 978-3-319-54398-7. DOI: 10.1007/978-3-319-54398-7_2. URL: https://doi.org/10.1007/978-3-319-54398-7_2.

[14] Jürgen H. Gross. "Tandem Mass Spectrometry". In: *Mass Spectrometry: A Textbook*. Cham: Springer International Publishing, 2017, pp. 539–612. ISBN: 978-3-319-54398-7. DOI: 10.1007/978-3-319-54398-7_9. URL: https://doi.org/10.1007/978-3-319-54398-7_9.

[15] Vera M. Mendes et al. "Validation of an LC-MS/MS Method for the Quantification of Caffeine and Theobromine Using Non-Matched Matrix Calibration Curve". In: *Molecules* 24.16 (2019). ISSN: 1420-3049. DOI: 10.3390/molecules24162863. URL: https://www.mdpi.com/1420-3049/24/16/2863.

[16] Daniel A. Abaye, Irene A. Agbo, and Birthe V. Nielsen. "Current perspectives on supercharging reagents in electrospray ionization mass spectrometry". In: *RSC Adv.* 11 (33 2021), pp. 20355–20369. DOI: 10.1039/D1RA00745A. URL: http://dx.doi.org/10.1039/D1RA00745A.

[17] Michiko Yoshitake. "What is the Work Function?: Definition and Factors that Determine the Work Function". In: *Work Function and Band Alignment of Electrode Materials: The Art of Interface Potential for Electronic Devices, Solar Cells, and Batteries*. Tokyo: Springer Japan, 2021, pp. 7–34. ISBN: 978-4-431-56898-8. DOI: 10.1007/978-4-431-56898-8_2. URL: https://doi.org/10.1007/978-4-431-56898-8_2.